Available online at www.sciencedirect.com
SCIENCE DIRECT®
International Journal of Heat and Mass Transfer 48 (2005) 5103–5111
International Journal of HEAT and MASS TRANSFER
www.elsevier.com/locate/ijhmt

Numerical simulation of two-fluid electroosmotic flow in microchannels

Yandong Gao, T.N. Wong *, J.C. Chai, C. Yang, K.T. Ooi

School of Mechanical and Aerospace Engineering, Nanyang Technological University, 50 Nanyang Avenue, Singapore 639798, Singapore

Received 13 January 2005; received in revised form 5 August 2005
Available online 7 October 2005

Abstract

This paper presents a numerical scheme for stratified two-liquid electroosmotic flows. The simulation results highlight that using the electroosmotic effects can control the interface location of a pressure-driven two-liquid flow. A finite volume method is used to solve the coupled electric potential equation and Navier–Stokes equation together.

The validity of the numerical scheme is evaluated by comparing its predictions with the results of the analytical solutions in the fully developed regions. The liquid–liquid interface developments due to the favorably and adversely applied electric field are examined.

Keywords: Two-fluid stratified flow; Electrical double layer; Electroosmotic effects; Numerical model; Two-fluid interface

1. Introduction

Electroosmosis refers to a liquid flow induced by an external electric field. When contacted with a polar solution, most surfaces acquire a finite surface charge density, which induces the electrically neutral solution to have a distribution of electrical charges. This high capacitance charged region of ions at the liquid/solid interface is known as the electrical double layer (EDL) [1]. EDL is primarily a surface phenomenon; its effect tends to appear when the typical channel dimension is of the order as the EDL thickness (Debye length). The thickness of EDL is dependent on the bulk ionic concentration and electrical properties of liquid, usually ranging from several nanometers to hundred. With the development of the biochip technology, electroosmosis has been widely used as a suitable pumping mechanism in the MEMS devices for chemical and biological analysis and medical diagnoses [2].

Two-liquid electroosmotic flows are encountered in a variety of microfluidics. However, the working liquid is required to be a conducting liquid with significant electrical conductivity which is called high EO mobility liquid. Low EO mobility liquids such as oil and ethanol cannot be pumped using the electroosmotic flow (EOF) due to the low electrical conductivity. In some biochemical analysis, the electroosmosis may be unsuitable directly for the water solutions. This is because that the voltage applied to the solutions can lead to undesirable problems, i.e., the electrochemical decomposition of the solute, the fluctuation of the pH of the buffer

* Corresponding author. Tel.: +65 790 5587; fax: +65 6792 4062.
E-mail address: mtnwong@ntu.edu.sg (T.N. Wong).

0017-9310/$ - see front matter © 2005 Elsevier Ltd. All rights reserved.
doi:10.1016/j.ijheatmasstransfer.2005.08.005

Nomenclature

e	elementary charge
E	electric field intensity
H	height of the channel
H_γ	Heaviside function
K	electric double layer parameter
k_b	Boltzmann constant
L	length of the channel
$\dot{m}_c$	current mass flowrate
$\dot{m}_{cor}$	mass preservation factor
$\dot{m}_d$	desired mass flowrate
n	multiplication factor
n_0	bulk concentration
N	total number of the mesh
t, t'	pseudo time
T	absolute temperature
u_j	velocity vector
u	velocity in x-direction
v	velocity in y-direction
V	electric voltage
x	coordinates
$\vec{x}$	position vector
z_0	valence of ions
α	property
γ	grid size related parameter
ε	electric permittivity
κ_D	Debye length
μ	viscosity
ρ	density
ρ_e	net electric charge density
ξ	level set function
ζ_w	zeta potential at the wall
ς, ς'	distance function
ϕ	total electric potential
φ	externally applied electric potential
ψ	electric potential due to surface charge

Subscripts

1	high EO mobility liquid
2	low EO mobility liquid
ref	reference quantity

Superscript

–	dimensionless quantity

solution and the generation of gases. Brask et al. [3] and Watanabe et al. [4], independently, proposed an idea to use the high EO mobility liquid as a driving mechanism to drag another liquid to avoid the above mentioned problem. A concept to control the interface location of a pressure driven two-liquid flow in a microchannel using electroosmotic flow effect was proposed by Wang et al. [5]. Adjusting the magnitude and direction of the electric field had successfully controlled the interface position between the two liquids.

In this work, we tested a numerical model for two-liquid electroosmotic flow in a microchannel. We simulate two immiscible liquids or two immiscible liquids with low diffusivity: a high EO mobility liquid at the bottom section and a low EO liquid at the upper section of the channel as shown in Fig. 1. When an electric flied is applied across the channel, two liquids are driven both by the pressure and the electroosmosis effects. The flow of the two liquid depends on the viscosity ratio, external electric field, electroosmotic characters of the high EO mobility liquid and the interfacial curvature between them.

In this article, the level set (LS) method [6–8] is used to capture the two liquids interface. The local mass

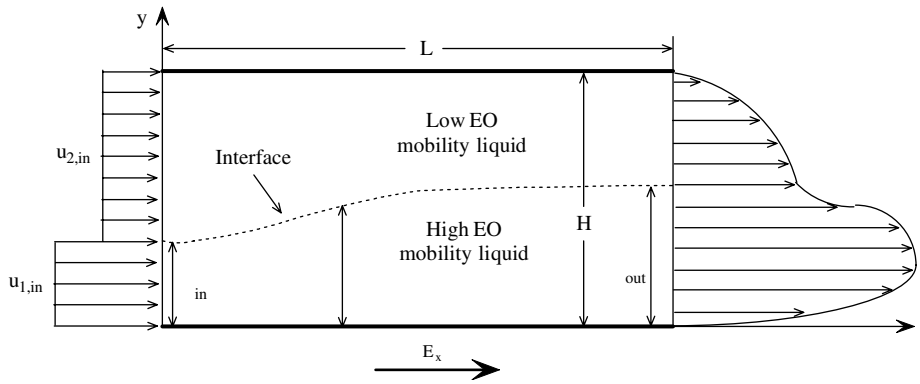

Fig. 1. Schematic of two-liquid electroosmotic between parallel plates.

correction scheme of Yap et al. [9] is used to ensure mass conservation of the two fluids at every cross-section as its flow along the microchannel.

2. Mathematical formulation

2.1. Governing equations

Fig. 1 shows the schematic of the problem considered in this article. The microchannel is filled with two (a high EO mobility and a low EO mobility) immiscible fluids. When an electric field is applied across the channel, the high EO mobility liquid is driven by electroosmosis. The high EO mobility fluid then drags the second fluid by the interfacial viscous force causing it to flow along the microchannel.

The steady, incompressible continuity and momentum equations for Newtonian fluids in Cartesian tensor notation for a two-phase flow problem can be written as

$$\frac{\partial(\rho u_j)}{\partial x_j} = 0 \tag{1}$$

$$\rho u_j \frac{\partial u_i}{\partial x_j} = \frac{\partial}{\partial x_j}\left(\mu \frac{\partial u_i}{\partial x_j}\right) - \frac{\partial p}{\partial x_i} + \frac{\partial}{\partial x_j}\left(\mu \frac{\partial u_j}{\partial x_i}\right) + \rho_e E_i \tag{2}$$

where u_j is the velocity vector, p is the pressure, ρ and μ are the density and viscosity appropriate for the phase occupying the particular spatial location, ρ_e is the net electric charge density and E is the electric field intensity. In this article, the capillary number is assumed to be large. As a result, the surface tension term is not included in Eq. (2). The electric field intensity is related to the electric potential, ϕ, by

$$E_i = -\frac{\partial \phi}{\partial x_i} \tag{3}$$

For small Debye length and small zeta potential, the electric potential can be further decomposed into the potential due to the charge acquired at the wall ψ, and the potential due to the externally applied electric field, φ [10]. This can be written as

$$\phi = \psi + \varphi \tag{4}$$

Furthermore, these two potentials are governed by Poisson equation and Laplace equation

$$\frac{\partial^2 \psi}{\partial x_j^2} = -\frac{\rho_e}{\varepsilon} \tag{5}$$

$$\frac{\partial^2 \varphi}{\partial x_j^2} = 0 \tag{6}$$

where ε is the electric permittivity appropriate for the phase occupying the particular spatial location. For a symmetric electrolyte, the net electric charge density, ρ_e, is given by the Boltzmann distribution based on the assumption of local thermodynamic equilibrium [11],

$$\rho_e = -2 z_0 e n_0 \sinh\left(\frac{z_0 e \psi}{k_b T}\right) \tag{7}$$

where z_0 is the valence of ions, e is the elementary charge, n_0 is the bulk concentration appropriate for the phase occupying the particular spatial location, k_b is the Boltzmann constant and T is the absolute temperature.

2.2. Boundary conditions

The boundary conditions for the velocities, electric potential due to externally applied electric field and electric potential due to the charges on the wall are

Inlet ($x = 0$)

$$\text{Velocities:}\quad u = \begin{cases} u_{1,\text{in}} & y \leqslant \delta_{\text{in}} \\ u_{2,\text{in}} & y > \delta_{\text{in}} \end{cases}, \quad v = 0 \tag{8a}$$

$$\text{Electric potentials:}\quad \phi = V_{\text{in}}, \quad \partial\psi/\partial x = 0 \tag{8b}$$

Outlet ($x = L$)

$$\text{Velocities:}\quad \partial u/\partial x = 0, \quad \partial v/\partial x = 0 \tag{8c}$$

$$\text{Electric potentials:}\quad \phi = V_{\text{out}}, \quad \partial\psi/\partial x = 0 \tag{8d}$$

Wall ($y = 0$)

$$\text{Velocities:}\quad u = 0, \quad v = 0 \tag{8e}$$

$$\text{Electric potentials:}\quad \partial\varphi/\partial y = 0, \quad \psi = \zeta_w \tag{8f}$$

Wall ($y = H$)

$$\text{Velocities:}\quad u = 0, \quad v = 0 \tag{8g}$$

$$\text{Electric potentials:}\quad \partial\varphi/\partial y = 0 \tag{8h}$$

Interface ($\xi = 0$)

$$\text{Electric potentials:}\quad \psi = 0 \tag{8i}$$

where u is the velocity in x-direction and v is the velocity in y-direction. V_{in} is the electric voltage at the inlet, V_{out} is the electric voltage at the outlet. ζ_w is the zeta potential at the wall contacting with the high EO mobility fluid. It is assumed that the wall in contact with the low EO mobility fluid does not acquire charges and interface does not touch the wall. Therefore, we do not specify the boundary condition of ψ, at the wall ($y = h$). Instead, we specify the condition of ψ at the interface ($\xi = 0$). In the framework of the model, it is also assumed that there is no charge concentration at the fluid–fluid interface. The situation, where the interface holds certain electric charge, will be considered in the future work. It is assumed two uniform velocities at the inlet for two liquids. $u_{1,\text{in}}$ is the inlet velocity for the high EO mobility liquid and $u_{2,\text{in}}$ for the low EO mobility liquid. The interface position of the interface, δ_{in}, is prescribed if Y-shape microchannel used.

We define the reference density as ρ_{ref} and viscosity as μ_{ref}. Then we non-dimensionalize the variables by scaling the length by the channel height H, the potential

φ by the value of the potential applied at the inlet V_{in}, the potential ψ by $(k_bT)/(z_0e)$, the velocity by $V_{in}\varepsilon k_bT/Hz_0e\mu_{ref}$ and the pressure by $\rho_{ref}(V_{in}\varepsilon k_bT/Hz_0e\mu_{ref})^2$. Eqs. (1), (2), (5), (6) and (7) can be rewritten as the dimensionless form, respectively

$$\frac{\partial(\rho\bar{u}_j)}{\partial\bar{x}_j}=0 \tag{9}$$

$$Re\bar{u}_j\frac{\partial\bar{u}_i}{\partial\bar{x}_j}=\frac{\partial}{\partial\bar{x}_j}\left(\bar{\mu}\frac{\partial\bar{u}_i}{\partial\bar{x}_j}\right)-Re\frac{\partial\bar{p}}{\partial\bar{x}_i}+\frac{\partial}{\partial\bar{x}_j}\left(\bar{\mu}\frac{\partial\bar{u}_j}{\partial\bar{x}_i}\right)+K^2\bar{\rho}_e\frac{\partial\bar{\varphi}}{\partial\bar{x}_j} \tag{10}$$

$$\frac{\partial^2\bar{\psi}}{\partial\bar{x}_j^2}=K^2\sinh(\bar{\psi}) \tag{11}$$

$$\frac{\partial^2\bar{\varphi}}{\partial\bar{x}_j^2}=0 \tag{12}$$

In above equations, Re is the Reynolds number defined as $Re=\rho_{ref}V_{in}\varepsilon k_bT/z_0e\mu_{ref}^2$, K is the EDL parameter defined as $K=H/\kappa_D$, where $\kappa_D=(\varepsilon k_bT/2z_0^2e^2n_0)^{1/2}$ is the Debye length.

2.3. Properties

The properties are calculated using

$$\alpha=(1-H_\gamma)\alpha_1+H_\gamma\alpha_2 \tag{13}$$

In Eq. (13), α can be the density, viscosity or electric permittivity. The Heaviside function H_γ is related to the normal distance from the interface and is calculated using [6]

$$H_\gamma=\begin{cases}0, & \xi<-\gamma\\ \dfrac{\xi+\gamma}{2\gamma}+\dfrac{1}{2\pi}\sin\left(\dfrac{\pi\xi}{\gamma}\right), & |\xi|\leqslant\gamma\\ 1, & \xi>\gamma\end{cases} \tag{14}$$

In Eq. (14), γ is related to the grid size and is usually taken as a factor of the grid spacing. The exact choice of γ will be explained in Section 3. ξ is the distance function, which will be discussed in the following.

2.4. Distance function

In this combined formulation, an additional scalar variable, called the level-set function, is used to identify the distances from the interface between the two phases and the reference plane. The equation governing the evolution of the level-set function is

$$\bar{u}_j\frac{\partial\xi}{\partial\bar{x}_j}=0 \tag{15}$$

In the solution of the level-set function (Eq. (15)), any convenient reference value can be assigned to the interface. The values of ξ at all node points are then calculated based on the reference value at the interface. The level-set function ξ is the *normal* distance from the interface. It is therefore a distance function which satisfies $|\nabla\xi|=1$. The value of ξ at the interface is set to zero. As a result, ξ has opposite signs in the two phases. For this formulation to work properly, ξ must remain a distance function. However, this can only be ensured at the beginning of the iteration process where the location of the interface is assumed and the values of ξ at all nodes are specified. During the iteration process, the values of ξ are calculated using Eq. (15). Although the interface is still represented by the reference value, the other values of ξ might not be the distances from the interface. As a result, another scalar variable is defined and solved. This variable must be a distance function and has the same interface value as ξ. The "steady-state" solution of ς given in Eq. (16) satisfies the above requirements.

$$\frac{\partial\varsigma}{\partial t}=\mathrm{sign}(\xi)(1-|\nabla\varsigma|) \tag{16}$$

In Eq. (16), t is a *pseudo* time for the variable ς. Eq. (16) is subjected to the following initial condition.

$$\varsigma(\vec{x},0)=\xi(\vec{x}) \tag{17}$$

It is clear from Eq. (16) that the "steady-state" solution satisfies $|\nabla\varsigma|=1$. Thus, it is a distance function. The initial value (Eq. (17)) ensures that the interface value of ς is identical to the interface value of ξ. As a result, the "steady-state" values of ς are the distances from the interface. Although Eq. (16) ensures ς and thus ξ as the distance function, it suffers a significant drawback. It does *not* ensure the conservation of mass of the various phases. To ensure mass conservation at *each* cross-section, a local mass correction factor is defined and an additional equation is solved [9]. This is written as

$$\frac{\partial\varsigma'}{\partial t'}=\dot{m}_{cor} \tag{18}$$

In Eq. (18), t' and $\dot{m}_{cor}$ are pseudo-time (which can be different from the pseudo-time $\bar{t}$) and mass conservation factor, respectively. The local mass correction factor is

$$\dot{m}_{cor}=\mathrm{sign}(\xi_{ref})\frac{(\dot{m}_d-\dot{m}_c)}{\dot{m}_d} \tag{19}$$

where $\dot{m}_d$ and $\dot{m}_c$ are the desired mass flowrate and the most current local mass flowrate of the reference phase, respectively. Depending on the choice of the Heaviside function of the reference phase, the mass flowrate of the reference phase can be calculated using

$$\dot{m}=\begin{cases}\sum\rho_{ref}H_\gamma u\Delta A, & H_{\gamma,ref}=1\\ \sum\rho_{ref}(1-H_\gamma)u\Delta A, & H_{\gamma,ref}=0\end{cases}. \tag{20}$$

The summation is performed over a cross-section. In the absence of phase change, the desired mass flowrate is calculated using the *inlet* condition.

2.5. Solution procedure

The solution procedure can be summarized as follows:

1. Guess the locations of the interface.
2. Calculate the normal distances for all nodes from the interface.
3. Specify the properties for all nodes using Eqs. (13) and (14).
4. Solve the electric potentials given by Eqs. (11) and (12).
5. Solve the continuity and momentum equations given by Eqs. (9) and (10).
6. Solve for ξ (Eq. (15)) using the velocities obtained in Step 5.
7. Solve for the "steady-state" ς (Eq. (16)) using the values of ξ from Step 6 as the initial values.
8. Solve for the "steady-state" ς' (Eq. (18)) using the values of ς from Step 7 as the initial values.
9. Set $\xi(\vec{x}) = \varsigma'(\vec{x})$.
10. Repeat Steps 3–9 until the solution converges.

2.6. Numerical method

The continuity equation (Eq. (9)), momentum equation (Eq. (10)), electric potential equations (Eqs. (11) and (12)), the level-set equations (Eqs. (15), (16) and (18)) are special cases of a general transport equation

$$\rho\frac{\partial \Phi}{\partial t} + \rho u_j \frac{\partial \Phi}{\partial x_j} = \frac{\partial}{\partial x_j}\left(\Gamma \frac{\partial \Phi}{\partial x_j}\right) + S \tag{21}$$

where Φ, ρ, Γ and S are the dependent variables, density, diffusion coefficient and source term respectively. The finite-volume method of Patankar [12] is used to solve the transport equation given in Eq. (21). A staggered grid is used in this article. The scalar variables are stored at the centers of the control volumes, while the velocities are located at the control volume faces. In this article, the power-law of [12] is used to model the combined convection–diffusion effect in the momentum equations. The first-order upwind scheme is used to model the convection of the level-set equations. The SIMPLER algorithm is used to resolve the velocity–pressure coupling. The fully implicit scheme is used to discretize the transient term. The resulting algebraic equations are solved using the TriDiagonal Matrix Algorithm.

3. Results and discussions

3.1. Validation of the numerical scheme

The mathematical model presented in the previous section is validated by comparing with the exact solutions of Gao et al. [13]. Unless otherwise specified, the high EO mobility fluid is called fluid 1; while the low EO mobility fluid is called fluid 2. The high EO mobility fluid is also used to calculate reference values for non-dimensionalization purposes. As seen in Fig. 1, the two fluids flow between two parallel plates of length L separated by a distance H. The height of fluid 1 is the entrance of the channel, δ_{in}. When an external electric field, $-\partial\varphi/\partial x$, is applied along the channel, the electro-osmotic body force due to the presence of EDL causes the high EO mobility fluid to flow. The high EO mobility fluid drags the low EO mobility fluid along. The interface between two fluids evolves along the flow direction. The velocity profile and the interface position at every section change with the strength of the applied electric field, ions properties in the high EO mobility fluid and the zeta potential at the wall in contact with the high EO mobility liquid. Once fully developed, the velocity profile and the interface location become independent of the streamwise coordinate.

In modeling EO flow in microchannels, it is important that the EDL is captured accurately. The thickness of the EDL, $\kappa_{\text{D}} = (\varepsilon k_{\text{b}} T/2z_0^2 e^2 n_0)^{1/2}$, termed as Debye length, is in the order of 10 nm–1 μm. The region of varying potential extends to a distance of about $3\kappa_{\text{D}}$ before the potential has decayed to about 2% of its value at the surface [11]. On the other hand, the microchannels utilized in many lab-on-a-chip applications are between 1 μm and 100 μm. As a result, K is a big number and the electroosmotic forces are concentrated within a very thin region adjacent to a surface. Finer meshes near these affected regions are needed to capture the EDL forces accurately. In this article, piecewise-uniform fitted mesh [14] in the transverse direction is applied to resolve the EDL. The mesh is defined as

$$\bar{y}_i = \begin{cases} 3i\Delta/N & i \leqslant N/3 \\ \bar{y}_{i-1} + 3(1-\Delta)/2N & i > 2N/3 \end{cases} \tag{22a}$$

with

$$\Delta = \min\left\{\frac{1}{3}, \frac{4}{K}\ln N\right\} \tag{22b}$$

where N is the total number of the mesh. The piecewise-uniform mesh points in the region $4\kappa_{\text{D}}$ from the wall. In fact one-third of the mesh points are there, and so the EDL is resolved by this method. A typical mesh is shown in Fig. 2. In the following, γ in Eq. (14) is calculated as

$$\gamma = n\frac{3(1-\Delta)}{2N} \tag{23}$$

where n is an integrate number.

In the simulations, we fix the channel geometry $H = 100$ μm and $L = 150$ μm. The electric voltage at the inlet, V_{in}, is 0.75 V and at the outlet, $V_{\text{out}} = 0$. The reference quantities μ_{ref} and ρ_{ref} are 10^{-3} Pa s and

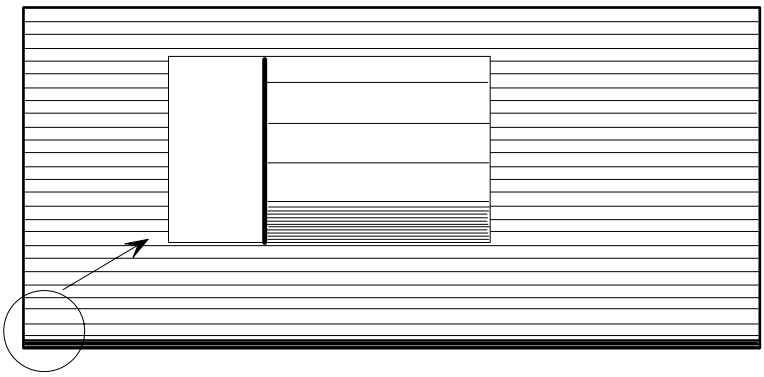

Fig. 2. Schematic of the piecewise-uniform fitted mesh in y-direction.

10^3 kg m^{-3}, respectively. At these conditions, the velocity scale is 9×10^{-5} m/s and the Reynolds number is about 3.6×10^{-3}.

For a set of given viscosity ratio (μ_2/μ_1), applied electric field, pressure gradient, the fully developed thickness of the high EO mobility fluid δ_{out}/H, depends on the volumetric flowrate ratio (q_2/q_1) of the two fluids. For this verification, fluid 1 occupies 30% of the channel at the inlet and the volumetric flowrate ratio is fixed such that both fluids occupy half of the channel in the fully developed region.

The values of other parameters in this case are chosen as: $K=200$, $\mu_2/\mu_1=10$, $\bar{\zeta}=0.2$. The inlet conditions are set such that the outlet is equally occupied by the two fluids. Fig. 3 shows the interface and the velocity profiles at five streamwise locations, when $N=120$ and $n=2$.

Table 1 shows the dimensionless thickness (δ_{out}/H) for various meshes. The errors are within 2% in all cases. At the outlet, in Fig. 3, a comparison is shown to the exact velocity profile [13]. Fig. 4 shows the detail comparisons of the fully developed velocity profile obtained using various computational grids with the exact solution when $n=2$. The results presented in Fig. 4 show the decay of discretization error with increased the total grid number N. It can be seen that the exact solution is reproduced accurately.

Table 1
Interface position at the outlet for different mesh densities

N	δ_{out}/H	Relative error (%)
60	0.4931	1.42
90	0.5041	0.82
120	0.5028	0.56
150	0.5016	0.32

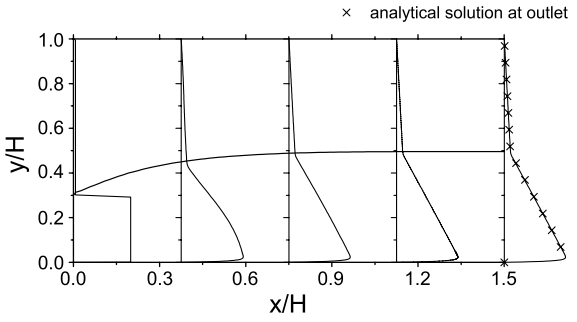

Fig. 3. Evolutions of velocity and interface profiles along x/H.

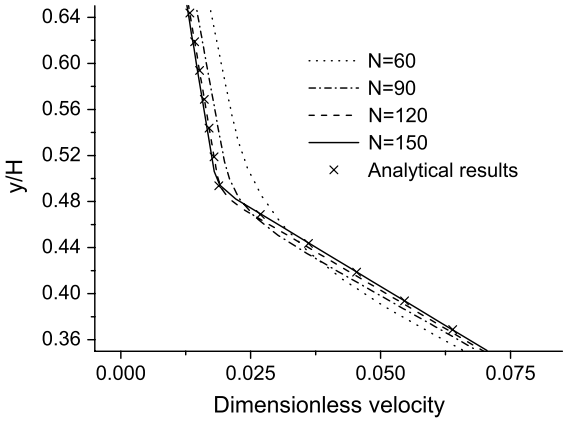

Fig. 4. Velocity profiles for various meshes.

Fig. 5 shows the comparisons of the fully developed velocity profiles obtained using four values of n with the exact solution when the total grid number $N=120$. Under the same total number of grid N, a small value of n corresponds to a smaller transient region for the properties in Eq. (13), the velocity profile becomes sharper.

From all of above results, we can conclude that the interface evolution between two fluids is well captured

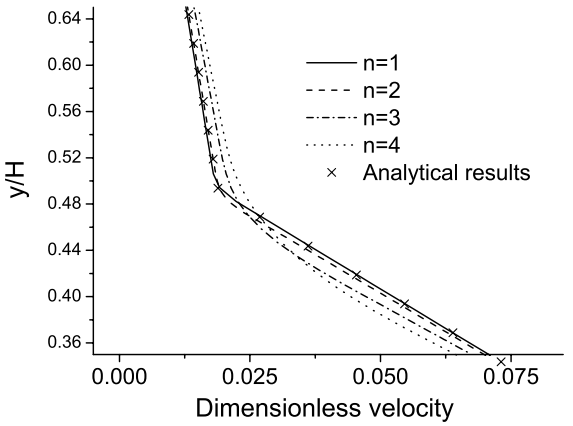

Fig. 5. Velocity profiles for various values of n.

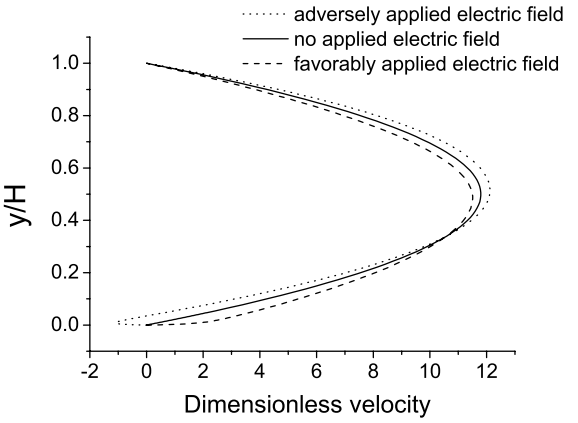

Fig. 7. The velocity profiles at outlet for $\mu_2/\mu_1 = 1$.

and this numerical method is suitable. In the following simulations, $N = 120$ and $n = 1$ are used.

3.2. Two-liquid EOF corresponding to various applied electric fields

In this section, the interfaces developments of two liquids due to various applied electric fields namely, favorably applied electric field and adversely applied electric field are examined. The focus of this problem is on the prediction of the interface evolution in the present of various external electric fields.

For a set of given viscosity ratio (μ_2/μ_1), volumetric flowrate ratio and pressure gradient, the fully developed thickness of the high EO mobility fluid δ_{out}/H, varies with the applied electric field. The values of parameters in this case are chosen as: $K = 200$, $\bar{\zeta} = 4$, and same volumetric flowrate $q_2/q_1 = 1$.

Figs. 6 and 7 show the evolutions of the interface and velocity profiles at the outlet for three different applied electric fields—no applied electric field, favorably and adversely applied electric fields, respectively. The favorable electric field is applied as $V_{in} = 0.75$ V and $V_{out} = 0$, while the adverse one is applied as $V_{in} = 0$ and $V_{out} = 0.75$ V. Under favorably applied electric field, the electroosmotic forces will drag the high EO mobility liquid to facilitate its flow in the same direction of the pressure gradient. But adversely applied electric field will generate an opposite electroosmotic force and work against the pressure-driven flow.

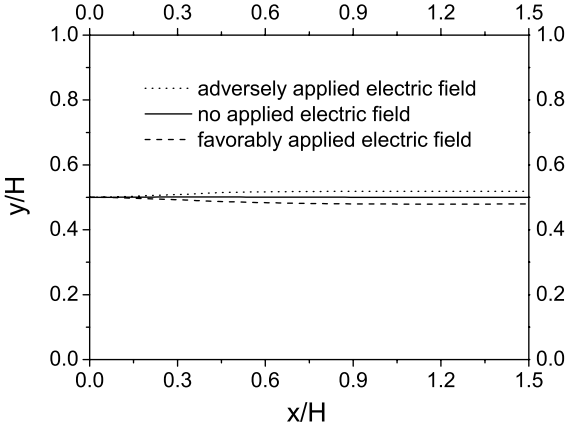

Fig. 6. The interface profiles along x/H for $\mu_2/\mu_1 = 1$.

For the pure pressure driven flow, the two liquids occupy half of the channel at the fully developed region (outlet) due to the same viscosity. As the electroosmotic force is concentrated in the EDL region close to the wall contacting with the high EO mobility liquid, the high EO liquid will flow faster in this region when a favorable electric field is applied. The average velocity of the high EO mobility liquid becomes faster. As the results, for the favorably applied electric field, the interface location at outlet becomes lower than the pure pressure driven flow. On the contrary, for the adversely applied electric fields, the high EO mobility liquid will bear an electroosmotic force against the flow direction. Apparently the high EO mobility fluid becomes more 'viscous' due to the adversely applied electric field. Therefore the high EO mobility liquid will occupy more portion of the channel than the pure pressure driven flow as shown in Figs. 6 and 7.

Figs. 8 and 9 show the evolutions of the interface and velocity profiles at the outlet for the three different applied electric fields when the viscosity ratio $\mu_2/\mu_1 = 10$. Since liquid 2 is more viscous, to achieve the same volumetric flowrates, the more viscous fluid has to spread to a large portion as compare to the case when $\mu_2/\mu_1 = 1$ (Fig. 6). The results further indicate that by adjusting the magnitude and direction of electric field, electroosmosis effect can be used to control the interface location of a pressure driven flow in microfluidics channels.

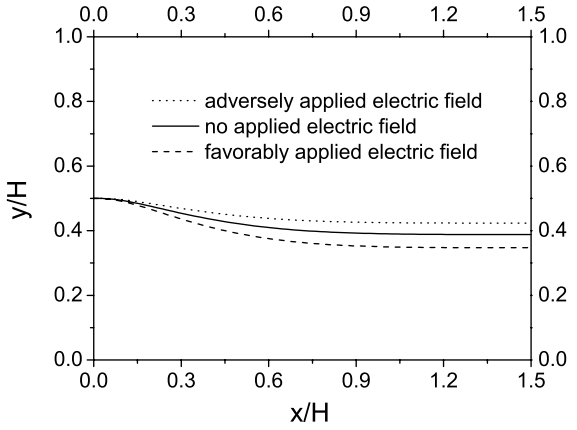

Fig. 8. The interface profiles along x/H for $\mu_2/\mu_1 = 10$.

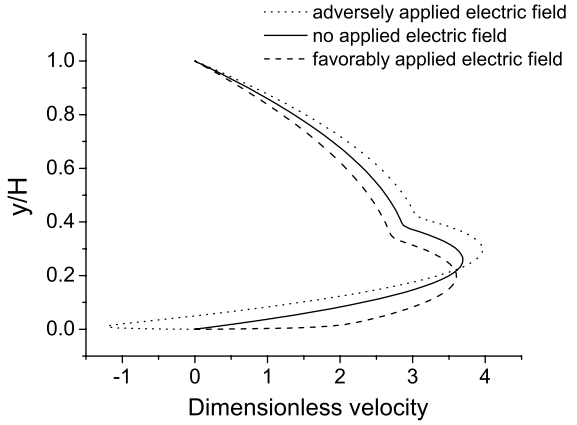

Fig. 9. The velocity profiles at outlet for $\mu_2/\mu_1 = 10$.

Comparing between Figs. 9 and 7 indicates that the velocity profiles of two-liquid flow are strongly dependent on the viscosity ratio μ_2/μ_1. When the viscosity ratio is high, the flow resistance of the low EO mobility liquid is high, resulting in a steeper velocity gradient in the interface, as shown in Fig. 9.

The velocities of two liquids can be considered as a linear combination of the electroosmotic flow and a pressure driven flow. In the cases of adversely applied electric field, the electroosmotic flow works against the pressure driven flow. Depending on the magnitude of the electric fields, reverse flow occurs when the electroosmotic force is strong enough as shown in Figs. 7 and 9.

Fig. 10 shows the interface and the velocity profiles at five streamwise locations for various applied electric field when $\mu_2/\mu_1 = 10$. It can be seen that the present procedure captures the interface location and resolve the EDL correctly.

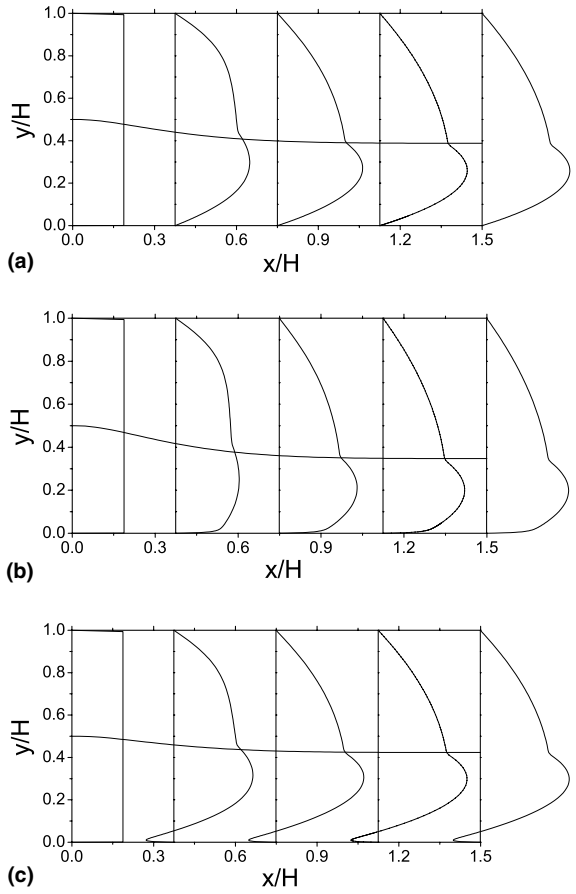

Fig. 10. Evolutions of velocity and interface profiles along x/H when $\mu_2/\mu_1 = 10$. (a) No applied electric field. (b) Favorably applied electric field. (c) Adversely applied electric field.

4. Concluding remarks

We presented numerical simulations results for two-liquid electroosmotic flow in straight channel. The simulations are performed for a specified inlet flowrate conditions and the electroosmotic forces are applied locally. The simulation results demonstrate the interface locations of a pressure-driven two-liquid flow in a microchannel can be controlled by using the electroosmotic flow effects. This concept has potential application for switching and cell sorting in bioanalytical systems.

References

[1] R.F. Probstein, Physicochemical Hydrodynamics—An Introduction, second ed., Wiley and Sons, New York, 1994, pp. 190–202.

[2] S. Zeng, C.-H. Chen, J.G. Santiago, et al., Electroosmotic flow pumps with polymer frits, Sensors Actuat. B 82 (2002) 209–212.

[3] A. Brask, G. Goranović, H. Bruus, Electroosmotically driven two-liquid viscous pump for no conducting liquids, in: Y. Baba et al. (Eds.), Micro Total Analysis Systems 2002, vol. 1, Kluwer Academic Publishers, 2002, pp. 145–147.
[4] M. Watanabe, H. Shirai, T. Hirai, Liquid–liquid two-layer electrohydrodynamic flow system, Sensors Actuat. B 94 (2003) 267–270.
[5] C. Wang, Y. Gao, et al., Interface control of pressure-driven two-fluid flow in microchannels using electroosmosis, J. Micromech. Microeng., in press.
[6] S. Osher, J.A. Sethian, Fronts propagating with curvature-dependent speed: algorithms based on Hamilton–Jacobi formulations, J. Comput. Phys. 79 (1988) 12–49.
[7] M. Sussman, P. Smereka, S. Osher, A level set approach for computing solutions to incompressible two-phase flow, J. Comput. Phys. 114 (1) (1994) 146–159.
[8] Y.C. Chang, T.Y. Hou, B. Merriman, S. Osher, A level set formulation of Eulerian interface capturing methods for incompressible fluid flows, J. Comput. Phys. 124 (2) (1996) 449–464.
[9] Y.F. Yap, J.C. Chai, et al., Numerical modeling of unidirectional stratified flow with and without phase change, Int. J. Heat Mass Transfer 48 (2005) 477–486.
[10] N.A. Patankar, H.H. Hu, Numerical simulation of electroosmotic flow, Anal. Chem. 70 (1998) 1870–1881.
[11] R.J. Hunter, Zeta Potential in Colloid Science, Principle and Applications, Academic Press, New York, 1981.
[12] S.V. Patankar, Numerical Heat Transfer and Fluid Flow, Hemisphere Pub. Corp., Washington, 1980, ISBN 0-07-048740-5.
[13] Y. Gao, N.T. Wong, C. Yang, O.T. Ooi, Two-fluid electroosmotic flow in microchannels, J. Coll. Interf. Sci. 284 (2005) 306–314.
[14] P. Farrell, A. Hegarty, J. Miller, et al., Robust Computational Techniques for Boundary Layers, Chapman & Hall/CRC, Boca Raton, 2000, ISBN 1-58-488192-5.